(197

Nuclear Science

Shielding Aspects of Accelerators, Targets and Irradiation Facilities – SATIF 7

Proceedings of the Seventh Meeting held at
Instituto Tecnológico e Nuclear (ITN)
Sacavém, Portugal
17-18 May 2004

Jointly organised by

Organisation of Economic Co-operation and Development
Instituto Tecnológico e Nuclear (ITN)
Radiation Safety Information Computational Center (RSICC)
The Division of Radiation Science and Technology of Atomic Energy Society of Japan

NEA No. 6005

NUCLEAR ENERGY AGENCY
ORGANISATION FOR ECONOMIC CO-OPERATION AND DEVELOPMENT

THE PISA EXPERIMENT: SPALLATION PRODUCTS IDENTIFIED BY BRAGG CURVE SPECTROSCOPY

F. Goldenbaum[1], V. Bollini[1], A. Bubak[1,2], A. Budzanowski[3], J. Cugnon[4], D. Filges[1], S. Förtsch[5], A. Heczko[6], H. Hodde[7], L. Jarczyk[6], B. Kamys[6], M. Kistryn[3], St. Kistryn[6], St. Kliczewski[3], J. Kisiel[2], A. Kowalczyk[6], P. Kulessa[1], H. Machner[1], A. Magiera[6], W. Migdal[6], K. Nünighoff[1], H. Ohm[1], N. Paul[1], B. Piskor-Ignatowicz[6], K. Pysz[1,3], Z. Rudy[6], R. Siudak[1,7], E. Stephan[2], D. Steyn[5], M. Wojciechowski[6], W. Zipper[2]

[1]Institut für Kernphysik, Forschungszentrum Jülich GmbH, Germany
[2]University Silesia, Katowice, Poland
[3]Institute of Nuclear Physics, INP-PAN Krakow, Poland
[4]University de Liège, Belgium
[5]IThemba LABS Faure, South Africa
[6]Jagellonian Univ. Krakow, Poland
[7]University Bonn, Germany

The PISA collaboration

Abstract

In the framework of spallation neutron sources and accelerator-driven systems, the international PISA (Proton-induced Spallation) collaboration has initiated measurements of total- and double-differential cross-sections for products of spallation reactions in a wide range of target nuclei (C-U) at the COSY proton accelerator in Jülich (Germany). The purpose is to study secondary particle production created in structural, window and target materials via proton beams up to 2.5 GeV of incident kinetic energy. Residual nuclei [H, He up to intermediate mass fragment (IMF)] production cross-sections are of great importance for estimating the damage to target and structure materials involving the planned spallation neutron sources, given that the lifetime of window and target materials is directly associated to those cross-sections. The demand for reliable theoretical predictions on production cross-sections is by no means satisfied by the models and codes that are available today. In this context, it is essential that reliable and comprehensive experimental data exist (especially for p energies beyond 1 GeV), which can serve as benchmarks for code development and validation. Data taken via Bragg curve spectroscopy and silicon detector telescopes for the reaction 1.9 GeV p + Ni(Au) will be discussed. Rather small lower detection thresholds involving Bragg Curve Detectors (BCDs) at ~0.5 MeV/nucleon were realised. With cooled silicon detectors, an energy resolution of about 0.4% was achieved and using BCDs excellent mass identification was obtained for all measured fragments from helium to silicon (e.g. $2 \leq Z \leq 14$). Kinetic energy spectra and angular distributions of emitted light ions and intermediate mass fragments will be shown.

Objective of the experiment

The experimental programme of the PISA project strives to measure total- and double-differential cross-sections for products of spallation reactions in a wide range of target nuclei (C-U), which is induced by protons of energies between 100 MeV and 2 500 MeV. These cross-sections and the quantitative knowledge on the interaction of medium- and high-energy protons with atomic nuclei are important for the following:

- Providing an extensive set of benchmark data in the GeV incident *p* energy range where few and divergent data exist [1,2,3].

- Understanding the complex reaction mechanism [3,4] via a comprehensive and systematic description of all nuclear reactions and measurement of kinetic energies as well as angular distributions of the ejectiles.

- Testing and increasing the reliability of physical models [2], which describe both the fast intra-nuclear cascade (INC) phase and the subsequent statistical decay from an equilibrated or thermalised hot nucleus.

- Developing new models for the description of highly energetic composite particles (there exist no models capable of reliably predicting production cross-sections, energy spectra or angular distributions).

- Planning and construction of high-intensity neutron spallation sources [6-10], given that the production cross-sections are of particular interest for studying radiation damage in target, window and structural materials. For example, helium is known to destroy the mechanical strength of solids, which limits the lifetime of both window and target (if solid). The production of tritium, which is a radioactive gas of considerable toxicity, has bearing on radiation safety provisions.

- Providing the Li, Be and B data for proton-induced reactions on light targets (up to Fe), which are of crucial importance for understanding the anomalous abundance of light elements in the cosmic rays (compared to the solar system) and astrophysical questions of nucleo-synthesis of light nuclei [11,12].

Regarding the dynamics of nuclear reactions, the following issues are not yet fully understood:

1. The approach to thermal equilibrium [3].

2. Competition between the sequential and simultaneous emission of fragments [13,14].

3. The production mechanism of intermediate mass fragments (IMF) and its relation to possible liquid-gas phase transition [15].

4. Expansion of the nucleus during excitation and subsequent decay [16].

The mass dependence of production cross-sections (for a full range of targets from carbon to uranium) should shed light on the competition of various mechanisms of interaction for protons with nuclei. It should also fill the current void of systematic data on the evolution of the production process as a function of bombarding energy and decaying system mass. Therefore, a primary task of the PISA

investigations is the determination of various IMF yields in their full kinetic energy range for several targets and incident proton energies. The PISA set-up, which allows for rather low (≤ 1 MeV/nucleon) energy thresholds, is an excellent experimental detection system.

Experimental set-up

Each of the eight detection arms (see Figure 1) in the PISA experiment consists of the following: two multi-channel plates (MCP) working as "start" and "stop" detectors for the time-of-flight measurement; a BCD [17] followed by three silicon detectors of 100, 300 and 4 900 μm thicknesses (for particle identification using ΔE-E techniques and kinetic energy measurement of intermediate-mass spallation products); and a set of double-layer scintillation detectors [fast and slow (phoswich)]. The purpose of the latter is to identify light-charged vaporation and spallation products such as *p*, *d*, *t* and He. [Currently, only the most forward detection arm (15°) and the most backward detection arm (120°) are mounted.) It will be shown that the TOF plus BCDs provide identification of light-heavy ions with masses up to 20-30 and kinetic energy starting from less than 1 MeV/amu.

Figure 1. Upper panel: Scattering chamber of PISA (October 2002) with the two full detector arms mounted at 15° and 120° and equipped with Bragg curve (BG), channel plate (inside chamber) and phoswich (PH) detectors. Lower panel: A detection arm in detail.

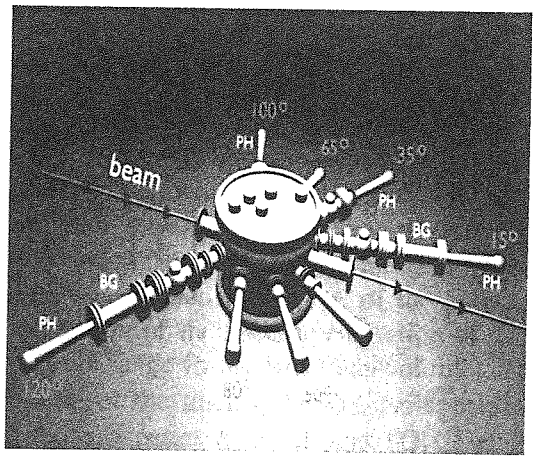

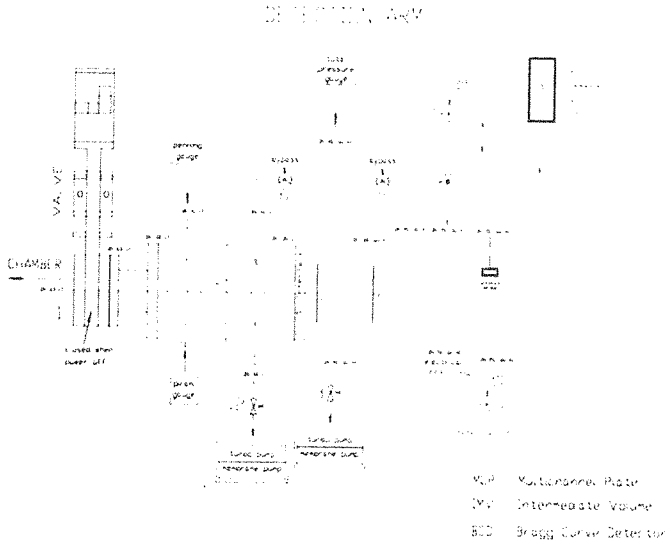

Channel-plate detectors

The telescope for the time-of-flight measurement is composed of two MCP detectors in the Chevron configuration. The channel plates were manufactured by the Galileo Corporation whereas we designed a suitable housing ourselves [18] (see the left panel of Figure 2).

The particles, which are to be registered, pass through the 20-μg/cm^2 thick carbon foil and knock out some δ electrons. These electrons are accelerated towards the MCP in the electric field between the foil, accelerating grid and second channel plate. The particular voltages are chosen to obtain the highest multiplication factor in the channel plates (10^7) and the best signal-to-noise ratio. Experiments showed that our MCPs performed best at voltages of 2 000 V (between the first and second channel plates) and ~400 V (between the carbon foil and accelerating grid).

The timing properties of MCPs were measured at the accelerator of the Heavy Ion Laboratory in Warsaw, Poland where a few low intensity beams of various ions passed through a telescope of two such assemblies (spaced by 27.4 cm). The measured time-of-flight resolution is smaller than 400 ps.

Figure 2. Left panel: Assembly for particle detection with the multi-channel plate detector. Right panel: BCD used for spallation studies of the COSY internal proton beam.

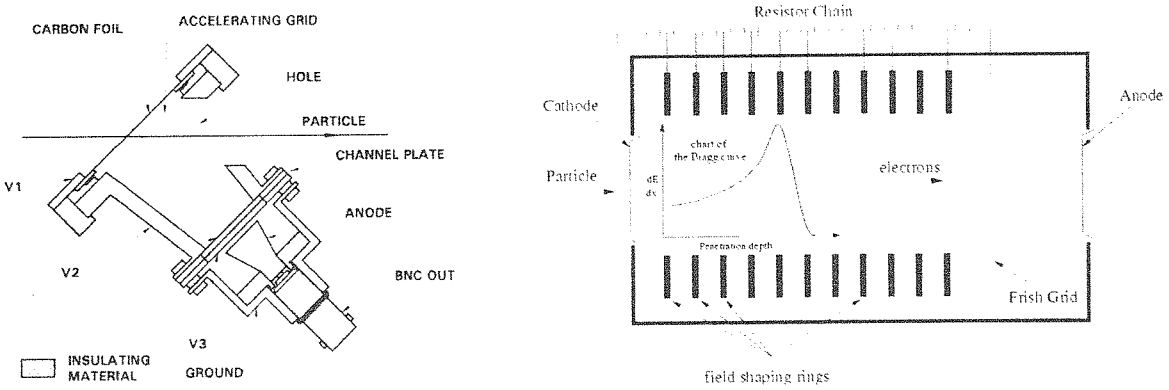

The Bragg curve detector

After successful utilisation of Bragg curve spectroscopy to identify highly-ionised particles [19,20], several detectors were built and used for various applications, which exploit Bragg curve characteristics. BCDs have allowed for the detection of fragments with high precision and over a broad range of nuclear charges with low registration thresholds [21-26]. This has been demonstrated in former experiments involving fragment production cross-sections for carbon with GeV proton beams [27,29].

Ref. [30] and a recently accepted paper [31] present the design of the BCD employed here and preliminary results of the first PISA test experiment. The design features of our BCD are very similar to those in Ref. [26] and references mentioned therein. Advantages (e.g. resistivity to radiation damage and insensitivity to minimally ionising particles) of BCDs compared to alternative detectors (e.g. gas-semiconductor ionisation chamber, solid state detectors, CsI(Tl) crystal scintillators) are outlined in Ref. [26]. The detector, as shown in the right panel of Figure 2, is an ionisation chamber with a gas volume of 22 cm in length and 5 cm in diameter. The detector is sealed off at its entrance by a 3-μm thick carbon-coated Mylar foil supported by a wire mesh, which will be operated by an anode (printed board) at ground potential and at the back end. The Frish grid, which defines the

ionisation sampling section (2 cm from the anode), is made of 20 μm gold-plated tungsten wires with 1 mm spacing. The voltage (>1 800 V) between the Frish grid and the entrance window is divided by a resistor chain, which is connected to nine field-shaping rings in order to maintain a homogeneous electric field over the active-detector volume. The particles enter through the cathode and leave an ionisation track parallel to the electric field.

For charged, non-relativistic particles, the Bethe-Bloch formula and its specific energy losses in a given medium can be simplified to $-dE/dx \sim cZ^2/E$, where Z, E are the atomic number and kinetic energy of the detected particle and c contains all relevant constants together with the quantities characterising the detector medium.

Since the energy loss per single collision is small, dE/dx increases slowly along the particle path. Only when the remaining energy is small does dE/dx increase rapidly, forming the Bragg peak (BP). The electrons along the track drift through the grid and are viewed as an anode current. The output signal from the anode as a function of time is proportional to the energy-loss distribution of the detected particle along its path through the detector. The atomic number of the incident-detected particle is therefore related to the maximum pulse height (corresponds to the BP) and the total kinetic energy of the particle (obtained from the integration over the total output signal). The detector is filled with iso-butane and is operated at a pressure of about 300 mb. Since iso-butane is characterised by a 30% lower effective-ionisation potential compared to argon [32] or the P10 mixture (90% argon, 10% methane), the number of released primary electrons is increased. Bragg curve spectroscopy principals are illustrated in the right panel of Figure 2, which shows a typical output signal of a BCD.

In addition to the usual charge identification by Bragg spectroscopy in the PISA experiment, an isotope separation for detected particles was achieved for elements up to nitrogen. The basic experimental information regarding the BCD was received from a VME-flash ADC module (CAEN model V729A, 40 MHz, 12 bit), which allowed for the data processing of about 1 000 sample Bragg curves per second. When the particle was stopped in the active chamber, apart from the measured TOF, the certain values were calculated from the pulse shape. The values include: the integral of the specific ionisation over the track (total kinetic energy E of the particle); the maximum of the BP, which was derived from the maximum of the specific ionisation of the ion (BP proportional to Z); the duration R (corresponding to the range in the BCD gas volume); and a partial integral from the specific ionisation at the beginning of the track ($\sim\Delta E/dx$). Isotope identification was performed by using the correlations between the parameters R, E, ΔE and TOF. Details on the BCD design can be found in Ref. [31]. For energies of emitted particles as low as 0.5 MeV/nucleon, the BCD is capable of measuring elemental distributions for fragments ranging from $Z = 2$ up to Si.

Results of the PISA experiment

COSY internal beam experiments allowed for the investigation of reactions induced by protons in thin targets (50-200 $\mu g/cm^2$), thus enabling the generation of cross-sections without the uncertainties (e.g. absorption and energy loss) that result from the propagation of reaction products in the target material. The multiple circulation of the beam in the COSY ring is used to compensate for the small reaction rate of beam protons with the thin target and to allow for measurement with optimal counting rates (1 000-2 000 s^{-1}) for a total intensity in the ring of about 10^{10}. The constant reaction rate is achieved by a negative back-coupling between the counting rate and the degree of overlapping of the proton beam with the surface of the target, which occurs via the controlled shifting of the beam in respect to the axis of the COSY beam line. Therefore, such an internal beam experiment offers a unique possibility to efficiently and precisely measure the cross-sections in thin targets.

Figure 3. Identification spectrum of emitted fragments in forward- (15°) and backward-mounted (120°) detection arms following 1.9 GeV p + Ni collisions

The maximum of the BP versus energy deposited in the detector. The helium ions are not highly visible in this representation but Li, Be and C up to Si lines can be distinguished. In addition, there are visible points in the area where Al and Si ions are expected. The identified products are indicated.

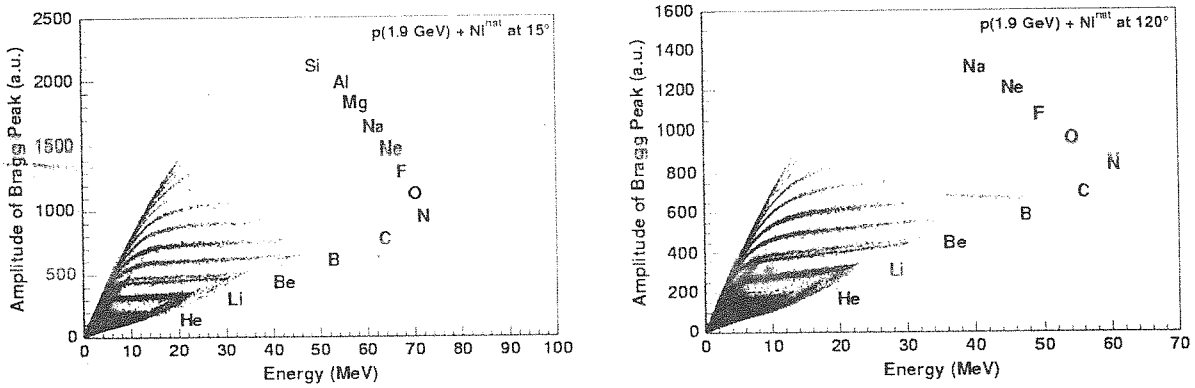

In a recently performed experiment (1.9 GeV p + Ni[Au]) involving BCDs, we observed an unambiguously identified charge of fragments from helium up to silicon (i.e. up to $2 \leq Z \leq 14$) and only a small amount of heavy fragments prevented us from finding the upper limit of the charge for emitted fragments. Figure 3 illustrates this phenomenon by showing the identification spectrum (BP versus energy E deposited in the gas volume) for the reaction 1.9 GeV p + Ni at the fragment emission angles of 15° (left panel) and 120° (right panel). Events with the same nuclear charge are located in branches parallel to the energy (range) axis and correspond to the particles stopped inside the BCD. The distinction of the charge is visible in the ranges of $2 \leq Z \leq 14$ and $2 \leq Z \leq 11$ at 15° and 120°, respectively. Most energetic particles with $Z \leq 6$ at 15° and $Z \leq 4$ at 120° have a range larger than the length of the BCD. This effect is quite visible in Figure 3, where the branch returns beyond the punch-through points (decreasing the energy deposited inside the BCD and the amplitude of BP). The slight slope in the BP amplitude, as a function of energy, was reported in earlier works and is caused by re-combination of the electrons and inefficiency of the Frish grid [27].

The rather good separation of elements (here shown for $3 \leq Z \leq 12$) is demonstrated in Figure 4, which is essentially a projection of the data in Figure 3 onto the axis denoting the Bragg peak. The resolution of charge distribution ΔZ was found to be between 10% and 12% per amu for peaks where isotopes were not distinguished, and 14% for Be where the isotopical structure was visible.

The measured range of kinetic energies is limited by lower- and upper-registration thresholds as demonstrated in the energy distributions shown for the reaction in Figure 5 (ejectiles emitted at 120° and 15° angles). The lower threshold is related to the energy losses of the emerging fragments in the target material and the BCD window foils to be penetrated. In Figure 3, the merging of the loci formed by the IMFs at the lowest energy (less than 1 MeV/nucleon) results from particles with energies that are too insufficient to form a BP in the counter. The upper registration threshold results from the finite active depth of the BCD, which mainly depends on the used gas and its pressure. The measured energy depends on the registered isotope and it is different for the forward and backward angles as Figure 5 illustrates for the reaction 1.9 GeV p + Ni. Note that the kinetic energy of particles emitted is larger in the case of forward angles than backward angles. Even for relatively heavy ejectiles (^{11,12,13,14}C and ^{13,14}N) emitted in a forward direction at 15° (shown in Figure 5, right panel), the kinetic energies were slightly higher than

Figure 4. Separation of elements by projection of Figure 3 (1.9 GeV p + Ni, 15°) onto the axis representing the BP. To effect the projection, a cut in the kinetic energy of particles was performed at $1.3 \leq E_{kin} \leq 3$ MeV/N.

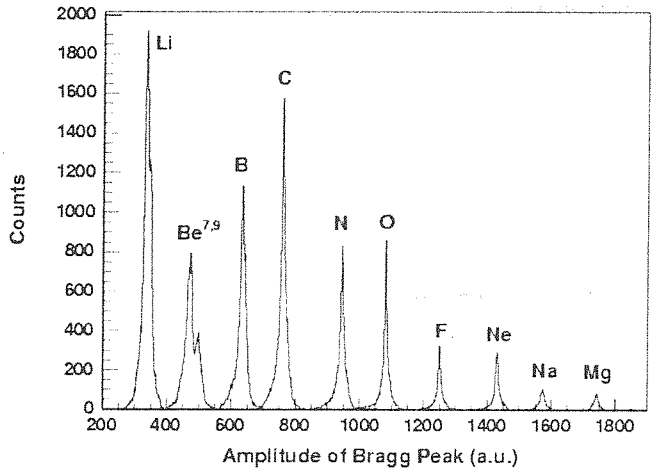

Figure 5. Left panel: Energy of different isotopes as identified by Figure 3 (1.9 GeV p + Ni, 120°) in combination with information from TOF. The spectra shown are neither corrected for detection efficiency nor normalised to absolute cross-sections. Right panel: Same as left but for 15°.

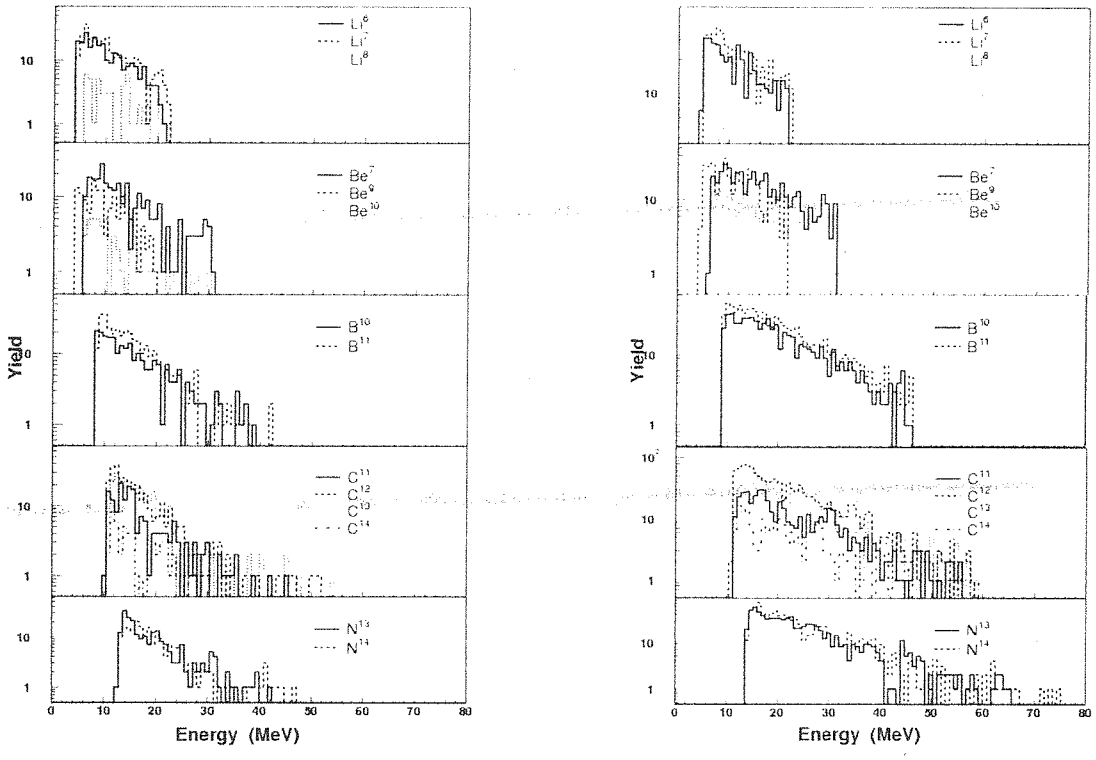

for particles emitted in a backward direction (Figure 5, left panel). The energy spectra shown are preliminary, since thus far no correction for detection efficiency has been considered and the absolute normalisation of the double differential cross-sections is still lacking. The Coulomb threshold within the energy spectra of fragments produced in p + Ni and p + Au collisions is expected at well above the

registration threshold of the BCD presented in this work, $E_{kin} \approx$ 2-3 MeV/nucleon. Consequently, in using the BCD, the maximum of the kinetic energy spectra due to the Coulomb barrier was clearly identified.

The fragment energies were corrected for energy loss via foils in front of the BCDs and entrance windows. The low energy cut-off arises from detector thresholds (~0.5 MeV/u) and energy loss via the foils. The correction for the efficiency of MCPs as a function of mass and energy was taken into account.

It is observed in Figures 5 and 6 that the slope of the energy spectra at 120° is steeper than at 15°. This indicates that the temperature extracted from the slope of the energy spectra should decrease as the detection angle increases. The fragment energy spectra were therefore fitted using a moving-source fit [28], which allows for an estimate of the temperature T. Example energy spectra of ^{10}B, ^{11}B, ^{13}N and ^{14}N isotopes and moving-source fits are shown in Figure 6. Extracted T values are around 4-7 MeV for backward and forward angles [28].

Figure 6. Energy spectra of ^{10}B, ^{11}B, ^{13}N and ^{14}N isotopes from 1.9 GeV p + Ni reaction observed at 15° and 120°

The identification of the isotopes was done by means of BCD spectroscopy combined with the time-of-flight method. The spectra shown are corrected for MCP efficiency. The solid lines represent moving-source fits.

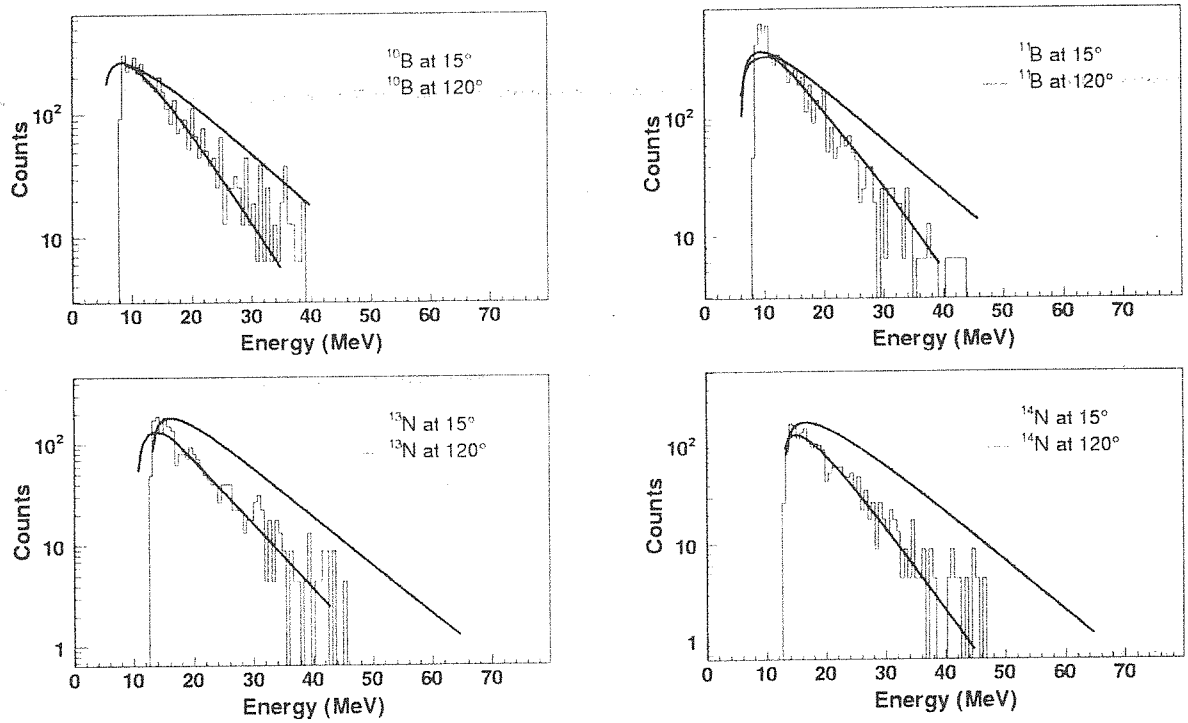

After selecting an element of given Z in the Bragg curve identification spectrum (Figure 3), an isotope separation or mass identification of the emitted fragments is possible due to different time-of-flights for different isotopes. The isotope separation was done by combining the information from MCPs (time-of-flight) and BCD (energy deposited inside the BCD), allowing for the separation of the following isotopes: ^{6}Li, ^{7}Li, ^{8}Li-^{7}Be, ^{9}Be, ^{10}Be-^{10}B, ^{11}B-^{11}C, ^{12}C, ^{13}C, ^{14}C, ^{13}N and ^{14}N. Note that due to the lack of ^{8}Be an isotopic separation is possible for ^{7,9}Be ions, even using the information provided in Figure 3 alone (i.e. without TOF knowledge).

Representatives of mass identification for isotopes up to ^{14}N are shown in Figure 7 for the 15° case.

Figure 7. The mass identification spectra for the 1.9 GeV p + Ni reaction products measured at 15°, which were obtained via the projection of mass distributions along the centres of gravity of ^{7}Li, ^{9}Be, ^{11}B, ^{11}C and ^{14}N

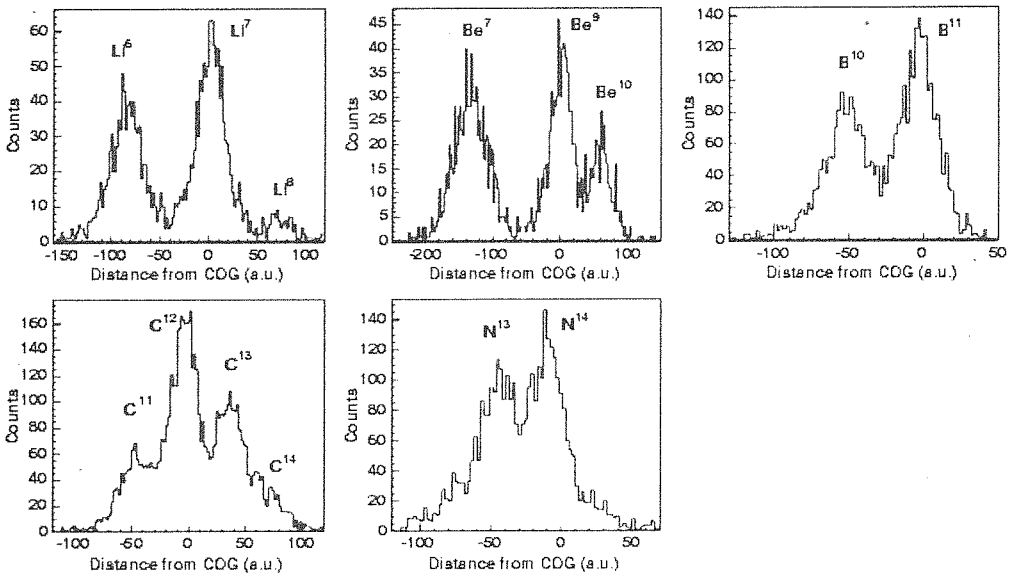

The second method of isotope identification consists of using Si-detector telescopes cooled down to -10°C. In fact, the telescope at 35° and 100° with respect to the proton beam consisted of the following four Si detectors: 50, 100, 400 and 3 000 μm and 20, 50, 100 and 400 μm, respectively. Excellent mass identification of all simultaneously measured fragments from helium to carbon was obtained as shown in Figure 8 for ejectiles emitted from p + Ni collisions at 1.9 GeV and 35°. The yield ratios of ^{7,9,10}Be and ^{8,10,11}B (see Figure 8) roughly reproduce the ones published in Ref. [29].

Figure 8. Mass identification spectrum of ejectiles emitted from p + Ni collisions at 1.9 GeV and 35° with respect to the proton beam

Energy loss of the ejectiles in the first silicon detector (50-μm thick) is plotted versus energy loss in the second silicon detector (100 μm) of the cooled Si telescope. The helium (^{4}He and ^{6}He), lithium (^{6}Li, ^{7}Li, ^{8}Li), beryllium (^{7}Be, ^{9}Be, ^{10}Be), boron (^{10}B, ^{11}B) and carbon (^{11}C, ^{12}C, ^{13}C) ions are well-separated. There are also visible individual points in this part of the figure where N ions are expected.

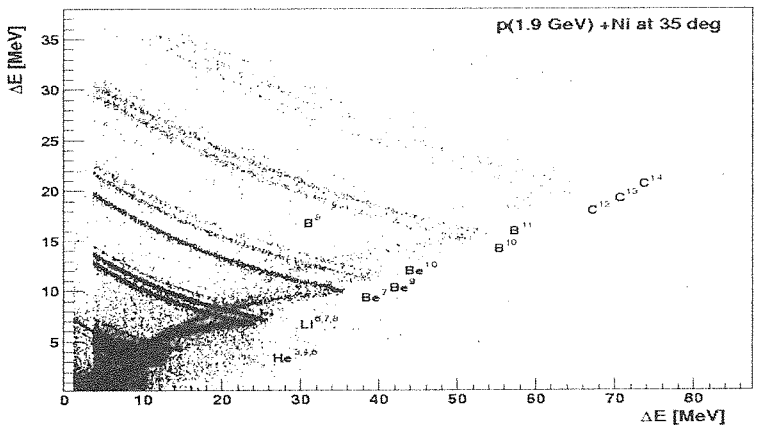

Conclusion

The aim of the current campaign is to check, revise and improve the predictive power of nuclear reaction models for spallation-source and astrophysics-relevant data and to identify existing INC/evaporation code deficiencies. The measurements on intermediate-mass fragments are considered as important experimental benchmark data for the development and testing of reliable new models. These models are capable of describing the emission of composite particles' high-energy component, which is produced in GeV reactions.

The PISA experiment at COSY-Jülich was consulted to validate models on reaction cross-sections, reaction probabilities, charged particle production cross-sections and angular and energy distributions following 1.9 GeV-proton induced reactions on thin C, Ni and Au targets. In summary, the experiment showed that in using the proposed technique, we are able to measure the products of proton-nucleus collisions with Z-identifications up to $Z = 16$ and to identify isotopes for masses up to 13-14 with particularly low energy thresholds of 0.5 MeV/A. The next beam time for PISA is requested for early 2004. Thinner films for the entrance windows are desired in order to reduce the energy loss. The most restrictive model tests are provided by data from exclusive experiments. Therefore, coincidence measurements (high-energy protons with other charged particles) are planned. A comprehensive comparison of the experimental data with the Monte Carlo predictions will be the subject of a forthcoming publication.

Acknowledgements

The excellent proton beam at COSY and the assistance provided by the COSY team were much appreciated. The project described in greater detail in Refs. [17,18,31,33] is supported by the EU-LIFE programme, the BMBF-Verbundforschung, the EU HINDAS project FIS5-1999-00150 and the EU TMR project ERB-FMRX-CT98-0244.

REFERENCES

[1] Enke, M., *et al.*, "Evolution of a Spallation Reaction: Experiment and Monte-Carlo Simulation", *Nucl. Phys.*, A657, 317 (1999).

[2] Filges, D., F. Goldenbaum, Y. Yariv, eds., "Models and Codes for Spallation Neutron Sources", *Proceedings of the 5th Workshop on Simulating Accelerator Radiation Environments (SARE-5)*, ISSN 1433-559X, ESS 112-01-T, OECD Headquarters, Paris, France, 17-18 July 2000 (2001).

[3] Herbach, C.M., *et al.*, "Light Particle Production in Spallation Reactions Induced by Protons of 0.8 to 2.5GeV Incident Kinetic Energy", *Proceedings of the International Conference on Nuclear Data for Science and Technology ND2001*, Tsukuba, Japan, Nuclear Data Center, JAERI, Tokai-mura, Naka-gun, Ibaraki-ken, 319-1195, Japan, 7-12 October 2001.

[4] Goldenbaum, F., *et al.*, "Decay Modes Induced by Light Particles", *International Workshop XXVII on Gross Properties of Nuclei and Nuclear Excitations*, Waldemar-Petersen-Haus, Hirschegg, Kleinwalsertal, Austria, 17-23 January 1999, GSI Darmstadt, ISSN 0720-8715, pp. 104-115 (1999).

[5] Pienkowski, L., *et al.*, "Vaporization and Multifragmentation in the Reaction 1.2GeV pbar + Cu and Ag.", *Phys. Lett.*, B472, 15 (2000).

[6] Appleton, B., *Proc. ICANS-XIII*, Report PSI 95-02, 814 (1995).

[7] Nagamiya, S., "JAERI-KEK Joint Project on High Intensity, Proton Accelerator", *9th Int. Conf. on Radiation Shielding*, Tsukuba, Int. Congress Center, Japan, 17-22 October 1999.

[8] *Spallation Neutron Source SNS*, Status Report, Oak Ridge National Laboratory, USA, See the web site http://www.ornl.gov/sns/.

[9] *The ESS Project*, Vol. III, Technical Report, ISBN 3-89336-303-3 (2002).

[10] Goldenbaum, F., D. Filges, "The ESS Future Project: Research with Neutrons, MESON2002", *7th International Workshop on Meson Production, Properties and Interaction of Mesons*, Cracow, Poland, 24-28 May 2002, World Scientific, L. Jarczyk, A. Magiera, C. Guaraldo, H. Machner, eds., ISBN 981-238-160-0, pp. 269-280 (2002).

[11] Reeves, H., *Rev. Mod. Phys.*, 66, 193 (1994).

[12] Silverberg, R., C.H. Tsao, *Phys. Rep.*, 191, 351 (1990).

[13] Botvina, A.S., D.H.E. Gross, "Sequential or Simultaneous Multifragmentation of Nuclei", *Phys. Lett.*, B344, 6 (1995).

[14] Moretto, L.G., *et al.*, "Are Multifragment Emission Probabilities Reducible to an Elementary Binary Emission Probability", *Phys. Rev.*, 74, 1530 (1995).

[15] Pochodzalla, J., *et al.*, "Probing the Nuclear Liquid-gas Phase Transition", *Phys. Rev. Lett.*, 75, 1040 (1995).

[16] Botvina, A.S., A.S. Iljinov, I.N. Mishustin, J.P. Bondorf, R. Donangelo, K. Sneppen, "Statistical Simulation of the Break-up of Highly Excited Nuclei", *Nucl. Phys.*, A475, 663 (1987); *Nucl. Phys.*, A448, 753 (1986); *Nucl .Phys.*, A444, 460 (1985); *Nucl. Phys.*, A443, 321 (1985).

[17] The PISA Coll., *IKP/COSY Annual Report 1999*, Jül-3744, ISSN0944-2952, p. 175ff (1999).

[18] The PISA Coll., *IKP/COSY Annual Report 2000*, Jül-3852, ISSN0944-2952, p. 172ff (2000).

[19] Schiessl, Ch., *et al.*, *Nucl. Instr. Meth.*, 192, 291 (1982).

[20] Gruhn, C.R., *et al.*, *Nucl. Instr. Meth.*, 196, 33 (1982).

[21] McDonald, R.J., *et al.*, *Nucl. Instr. Meth.*, 219, 508 (1984).

[22] Moroni, A., *et al.*, *Nucl. Instr. Meth.*, 225, 57 (1984).

[23] Westfall, G.D., *et al.*, *Nucl. Instr. Meth.*, A238, 347 (1985).

[24] Kotte, R., *et al.*, *Nucl. Instr. Meth.*, A257, 244 (1987).

[25] Kotov, A.A., *et al.*, *Exp. Technik der Phys.*, 36, 6, 513 (1988).

[26] Ochiishi, H., *et al.*, *Nucl. Instr. Meth.*, A369, 269 (1996).

[27] Andronenko, L.N., *et al.*, *Nucl. Inst. Meth.*, A312, 467 (1992).

[28] Bubak, Arek, PhD thesis, To be published (2003).

[29] Andronenko, L.N., *et al.*, *Nucl. Phys. Inst.*, Gatchina, Preprint 2217, NP-3-1998 (1998).

[30] Budzanowski, A., *et al.*, *IKP/COSY Annual Report 1999*, p. 176.

[31] Barna, *et al.*, *Nucl. Instr. Meth.*, A519, 610-622 (2003).

[32] Sauli, F., *Principles of Operation of Multiwire Proportional and Drift Chambers*, CERN 77-09 (1977).

[33] The PISA Coll., *IKP/COSY Annual Report 2001*, Jül-3978, ISSN0944-2952, p. 210ff (2001).